

DESIGN OF WING LEADING EDGE AGAINST BIRD STRIKE

M. Hakan Gülseven¹ Selim Gök² Zehra Toprak³
and Ahmet Güldağı⁴
Ankara Yıldırım Beyazıt University
Ankara, Turkey

Prof. Dr. Fahrettin Öztürk⁵
Turkish Aerospace Industries, Inc.
Ankara, Turkey
Ankara Yıldırım Beyazıt University
Ankara, Turkey

ABSTRACT

This study offers a variety of geometry designs in which the leading edge can emerge this situation with minimal damage if a bird strikes the wing leading edge. The hemispherical-ended cylinder model for bird geometries is used in the study. An optimization study is also made using the data obtained from the analysis results for these leading edges consisting of various geometries and materials, and the most suitable is selected. Results indicate that the most important parameters for the mass and deformation, which are the performance requirements, are the design geometry and the skin thickness.

Keywords — bird strike, optimization, SPH, leading edge

INTRODUCTION

The natural and human features of the world sometimes adapt wonderfully, while sometimes biological richness can cause serious problems in these human-made structures. One of the most important examples of this is bird strikes in aviation. This issue, which has a serious importance in the field of aviation, is constantly followed by engineers and scientists and solutions are tried to be produced. This situation causes significant loss of life and serious financial damage to aerospace industry. It is still a serious issue even with advanced technologies.

A bird strike occurs when a moving aircraft collides with an airborne avian creature (usually a bird or bat) or a group of such avian creatures. Other wildlife species, such as terrestrial mammals, are generally included in the term of bird strike. [Hedayati, 2016].

In order to prevent bird strike accidents, which are an important problem in aviation, studies are carried out and solutions are tried to be produced. These accidents cause significant loss of life and serious material damage to aircraft. Efforts are being made to minimize the damage and to reduce this effect in the air. The number of bird strikes reported to the FAA from US-registered aircraft between 1990 and 2019 was 227045 within the US and 4275 outside the

¹ Senior Design Project Student, Email: mustafahakangulseven@gmail.com

² Senior Design Project Student, Email: selimgok33@gmail.com

³ Senior Design Project Student, Email: zehraatopraak@gmail.com

⁴ Senior Design Project Student, Email: ahmet.guldagi@hotmail.com

⁵ Professor, Email: fahrettin71@gmail.com

US [Dolbeer, 2019]. Figure 1 shows the number of bird strikes reported. Looking at Figure 1, it can be seen that there has been a significant increase in bird strikes over the years. While the number of bird strike cases reported in 1990 was 1850, the number of bird strikes reported in 2019 was 17228. The cost of bird strike events was \$900 million between 1990 and 2019 [Dolbeer, 2019]. Considering unreported costs and bird strikes, the annual cost is estimated to be as high as \$500 million [FAA, FAQ, 2020]. It is estimated that this loss worldwide is 1.2 billion dollars [Allan,2000]. In addition, 292 people lost their lives as a result of bird strikes between 1988-2019. When we look at these material and moral losses, it is seen once again how important bird strikes can be. For this reason, aircraft manufacturers and airport operators have great responsibilities to prevent these accidents.

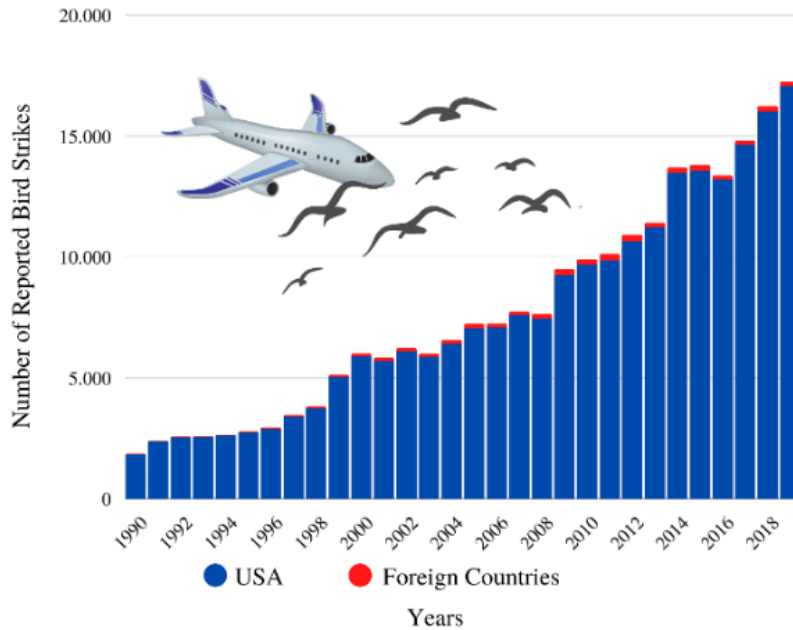


Figure 1: Bird strikes from US-registered aircraft in and outside the US between 1990 and 2019 [Dolbeer, 2019].

Different rates of damage have been recorded in different components of the aircraft in bird strike accidents. According to Boeing's statistics, 75% of bird strikes occurred on the engines and wings, as shown in Figure 2 [Nicholson, 2011]. Different designs are being studied in wing designs in order to ensure that aircraft wings come out with the least damage from bird strikes.

The wing is the part where the electronic components, hydraulic structures and fuel tank are located that enable the aircraft to take off and land. The bird must not damage the fuel tank and electronic components in the event of an impact. For these reasons, there are certification norms for aircraft manufacturers. According to CS 25,631 large airplanes should be designed to ensure safe flight and landing capability after striking an 1.814 kg (4 lb) bird when the speed of the airplane is equal to the design cruise speed at sea level or $0.85 V_c$ at 2438 m (8000 ft). There are no requirements for all structures on normal category aircraft. According to CS 23.775, each windshield and its supporting structure directly in front of the pilot must withstand impact equivalent to 0.91 (2 lb) kg of bird when the aircraft's speed is equal to the aircraft's maximum approach flap speed. Damage to the wing leading edge should be minimized to increase flight safety.

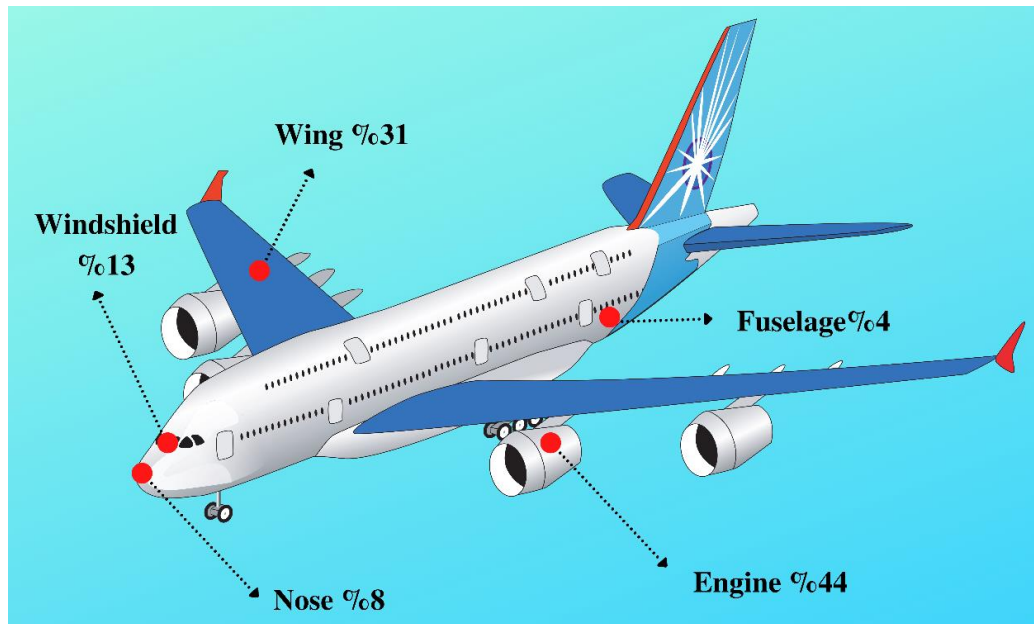


Figure 2: Bird strike damage ratios on an aircraft. Data is from Boeing [Nicholson, 2011].

As the first step in the study, the material model, geometry and finite element method of the model bird were investigated and the methods to be used were determined. Then, since bird strike is a problem that occurs at high speeds, the target material will behave differently and the modeling method to be used was chosen to accurately model this different behavior. In order to verify the analysis studies carried out in the project, a verification study was performed by comparing the results of the experiment on an aluminum plate in the literature. After the verification study, leading edge designs developed against bird strike in the literature were examined. An experimental design was made using the Taguchi Method. Factors and levels of experimental design were determined. After this experiment, analysis studies were carried out and the leading edge design that gave the lowest mass and gave the best performance was selected. The path followed in this study is summarized in Figure 3.

MATERIALS AND MODELS

Numerical Methods for Bird Model

There are four different finite element methods commonly used in impact analysis. These methods are Lagrange Method, Euler Method, Arbitrary Lagrange-Euler Method (ALE) and Smoothed Particle Hydrodynamics Method (SPH). In bird strike analysis, bird models are considered as a mixture of solid and liquid. While the Lagrange Method is generally used in the analysis of solid bodies, the Euler Method is used in the analysis of liquid bodies. Therefore, the ALE Method and the SPH Method are the most suitable to be used in bird strike analysis, but the ALE method was not preferred due to its difficulty in use. The SPH method is a widely used method that gives realistic results in bird strike analysis. In the SPH, each particle has its own mass, velocity and stress rate. The advantages of the SPH method are, firstly, that it does not require the elements to be interlocked, thus preventing the mesh from intermingling. Second, unlike the ALE method, it does not require many parameters to be considered and adjusted and is less complex [Hedayati, 2013]. The bird modeled by the SPH method is shown in Figure 4.

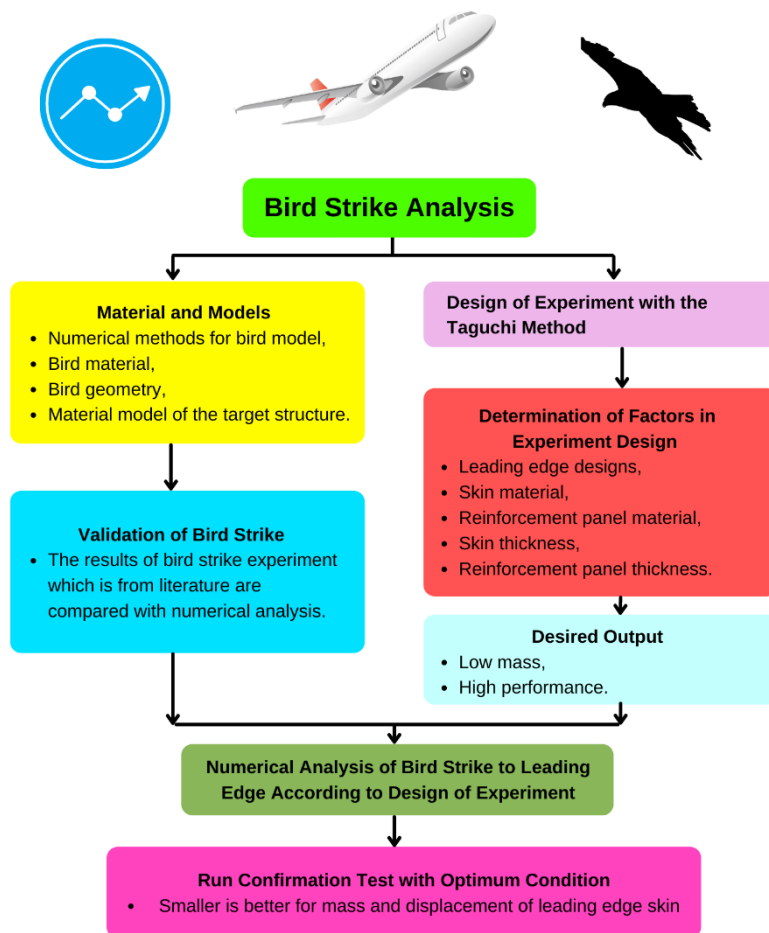


Figure 3: Steps followed throughout the bird strike analysis.

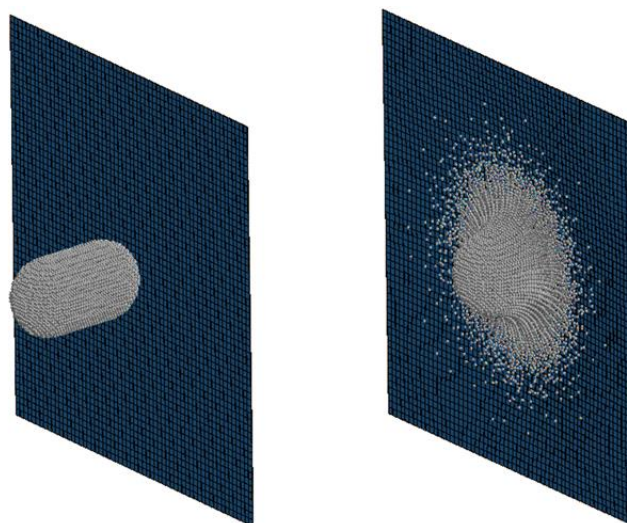


Figure 4: Bird modeled by the SPH method.

Bird Material

Bird impact of the material to make a proper analysis must be correctly modeled. Real birds are mostly consisting of water and air. Since the bird behaves as a fluid at high impact velocities, the hydrodynamic material model can be used for the bird model [Hedayati, 2016]. In the studies, the density of the bird model varies between 900 and 950 kg/m³. In addition, the International Bird Strike Research Group has developed a formula for the density of the alternative bird model to be used [Budgey, 2000]. In this study, biometric data was obtained by collecting bird species commonly seen in bird strike cases. The relationship between bird mass and density is given as:

$$\rho_{\text{bird}} = -0.063 \times \log_{10} m + 1.148 \quad (1)$$

In this equation, ρ_{bird} is the density of the model bird and m is its mass.

For hydrodynamic modeling, an equation of state (EOS) is usually used that describes the pressure-volume relationship with the water parameters at room temperature [Heimbs, 2011]. In bird strike studies, Polynomial EOS, Tabulated EOS, Murnaghan EOS and Gruneisen EOS were used. As a result of the literature study, it was decided to use the Gruneisen EOS in the modeling of bird material. The Gruneisen EOS is expressed as in Equation (2) for compressed material [Hedayati, 2016],

$$P = \frac{\rho_0 C_v^2 \mu \left[1 + \left(1 - \frac{\gamma_0}{2} \right) \mu - \frac{a}{2} \mu^2 \right]}{\left[1 - (S_1 - 1) \mu - S_2 \frac{\mu^2}{\mu + 1} - S_3 \frac{\mu^3}{(\mu + 1)^2} \right]^2} + (\gamma_0 + a \mu) E \quad (2)$$

and for expanding materials, it is expressed as in Equation (3).

$$P = \rho_0 C_v^2 \mu + (\gamma_0 + a \mu) E \quad (3)$$

In these equations,

C_v = the intercept of $v_s - v_p$ curve,

v_s = shock velocity,

v_p = particle velocity,

$S_1, S_2,$ ve S_3 = coefficients of the slope of the $v_s - v_p$ curve,

γ_0 = Gruneisen gamma,

a = the first order volume correction to γ_0 , and

E = internal energy density per unit initial volume.

For water, the values in the Gruneisen equation of state are used as $C_v = 1480$ m/s, $S_1 = 1.92$, $S_2 = 0$ and $\gamma_0 = 0.1$ [Hedayati, 2016].

Geometry of Bird Model

Birds, the beauties of our nature, have various shapes and geometries like other creatures. Birds are made up of bones, lungs, and other complex organs. For this reason, the load that will occur during impact may differ according to different bird species. Therefore, simplified models have been developed to analyze the bird strike effect. As seen in Figure 5, hemispherical-ended cylinder, flat-ended cylinder, ellipsoid and spherical shapes were used in bird strike analysis. The International Bird Strike Research Group stated that the diameter of the geometry would be one of the most critical parameters. During a test, it was noted that a certain part of the mass of the striking bird model was achieved and therefore diameter was an important parameter over length. In addition, the International Bird Strike Research Group has developed a formula for the diameter of the alternative bird model to be used, and suggested hemispherical-ended cylinder, flat-ended cylinder, and ellipsoid shapes [Budgey, 2000]. The biometric data in this study were obtained from various common bird species. The relationship between the mass and diameter of the bird is given as,

$$\log_{10} d = 0.335 \times \log_{10} m + 0.900 \quad (4)$$

In this equation, d represents the diameter of the model bird and m represents its mass.

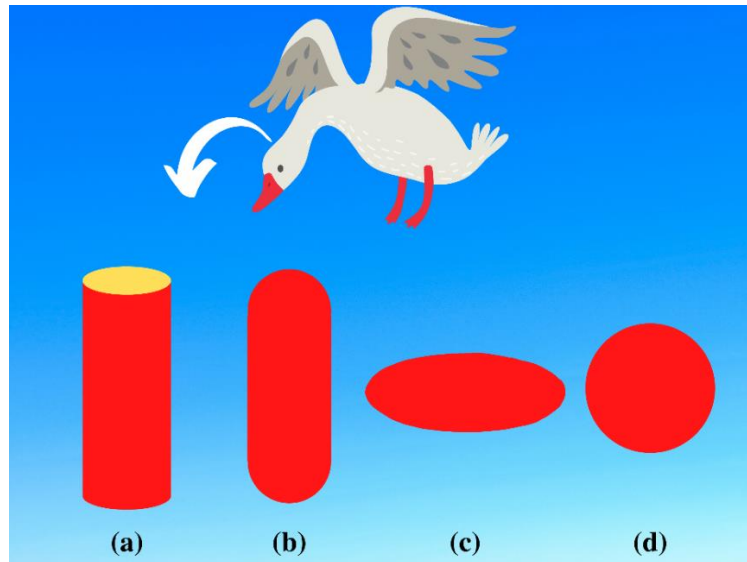


Figure 5: Frequently used geometries in bird strike analysis.

In this study, as in many other studies, the density of the bird was taken as 950 kg/m^3 , and a hemispherical-ended cylinder geometry with an aspect ratio of 2 was used. Hemispherical-ended cylinder bird model; the diameter of the model bird with an aspect ratio of 2 and a mass of 1.814 and 0.91 kg was calculated by using the mass, volume and density relationship below. The volume of the hemispherical-ended cylinder is as in Equation (5).

$$V = \frac{\pi d^3}{6} + \frac{\pi d^3}{4} = \frac{10\pi d^3}{24} \quad (5)$$

The relationship between mass, density and volume is as in Equation (6).

$$m = \rho V = \rho \left(\frac{10\pi d^3}{24} \right) \quad (6)$$

Using these relations, the diameter of the model bird with a mass of 1.814 kg was calculated as $d = 0.1134$ m, and the diameter of the model bird with a mass of 0.91 kg was calculated as $d = 0.090$ m. The dimensions of the birds are summarized in Figure 6.

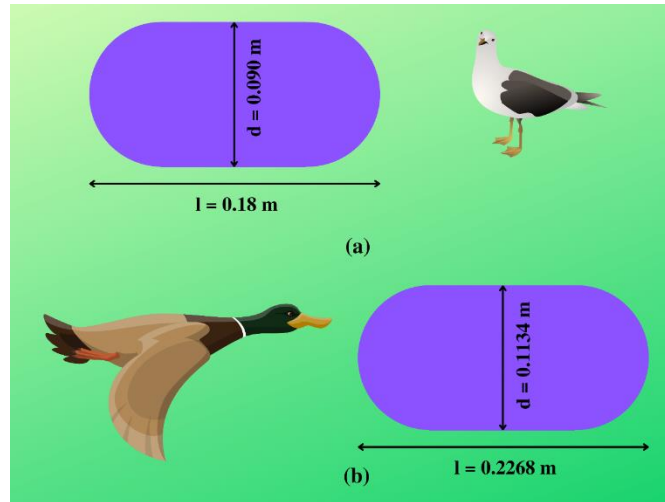


Figure 6: Calculated diameters and lengths for bird models. (a) Dimensions of the 0.91 kg bird model, (b) dimensions of the 1.814 kg bird model.

Material Model of Target Structure

For all products manufactured in the aviation industry, there are many forces that can affect the aircraft, such as lift, friction, sudden acceleration or deceleration, aerodynamic loads, loads exposed during landing, recoils during gunfire, and the vehicle's own weight. Because the safety and reliability of the aircraft operating under these forces are of paramount importance, the parts used in the aircraft must be able to perform as expected under all predetermined operating conditions. For this reason, the material properties and conditions of use of any part to be used in the aircraft should be examined in detail and all its properties should be known before the production phase. There are many different factors in these choices, which will be made according to the properties of the material. Especially in the aircraft industry, the most important of these factors is the mechanical properties of the material. Considering these mechanical properties, there are many types of metal materials used in the aerospace industry. The most commonly used materials in this field are stainless steels, nickel alloys, aluminum alloys, and titanium alloys.

Aluminum alloys stand out with their high strength/specific gravity ratio. Aluminum alloys find wide use in aircraft structures, especially in wing and fuselage skins. It has most of the need for materials with light weight, high strength and desirable properties for use in the aerospace industry. Many different types of aluminum alloys are used in the aircraft industry. The most commonly used alloys are the 2000, 6000, and 7000 series. There are many different types of aluminum, but some are more suitable for the aerospace industry than others.

As a result of the literature review, it has been seen that some important aluminum alloys are used on the leading edge of the aircraft wing. Some of the factors considered in leading edge materials such as skin, spars, ribs and stringers are fatigue strength, bending and torsional strengths, and resistance to hail damage. Considering all these, it is seen that different aluminum alloys are more suitable for each part. When the materials that can be used on the leading edge are examined, three important aluminum alloys appear. These are Al 2024-T3, Al 7050-T7451, and Al 7075-T6.

Many of the materials used in engineering have different properties. Bird strike is an event that takes place at high speeds. The behavior of materials during deformation depends on the

strain rate and temperature. Various models have been developed to accurately describe these behaviors. When these models are examined, the Johnson-Cook material model is one of the most common methods that allows the behavior of materials to be predicted at high strain rates. This model is expressed as in Equation (7) [Milani, 2009],

$$\sigma = [A + B\varepsilon_p^n] \left[1 + C \ln \left(\frac{\dot{\varepsilon}_p}{\dot{\varepsilon}_0} \right) \right] [1 - (T^*)^m] \quad (7)$$

In this equation, the terms can be defined as follows,

σ = equivalent stress response,

ε_p = equivalent plastic strain,

$\dot{\varepsilon}_p$ = equivalent plastic strain rate,

$\dot{\varepsilon}_0$ = normalizing reference strain rate,

A, B = strain hardening parameters,

C = dimensionless strain rate hardening coefficient,

n, m = power exponents of the strain hardening and thermal softening terms,

T^* = normalized temperature.

The Johnson-Cook parameters obtained using various methods are used in material modeling in bird strike analysis. The Johnson-Cook material model constants calculated for the different aluminum alloys used in the study are given in Table 1.

Table 1: The Johnson Cook and other material parameters of aluminum materials used in verification study and bird strike to leading edge analysis.

Parameters	Al2024-T3 [Buyuk,2013]	Al7050-T7451 [Huang,2020]	Al7075-T6 [Brar,2009] [Velamakuri,2018]	Al6061-T6 [Sumesh,2018]
Density	2770	2830 [Aurrekoetxea,2020]	2810	2700
Isotropic Elasticity				
Young Modulus	7.308×10^{10}	7.17×10^{10}	7.17×10^{10}	6.89×10^{10}
Poisson's Ratio	0.33	0.33 [Aurrekoetxea,2020]	0.33	0.33
Johnson Cook Material Parameters				
Initial Yield Stress, A	3.69×10^8	3.91×10^8	5.46×10^8	3.241×10^8
Hardening Constant, B	6.84×10^8	6.84×10^8	6.78×10^8	1.138×10^8
Hardening Exponent, N	0.73	0.436	0.71	0.42
Strain Rate Constant, C	0.0083	0.00959	0.024	0.002
Thermal Softening Exponent, m	1.7	2.0	1.56	1.34
Melt Temperature, t_m	501.85	620 [Matweb,2021]	635	652
Specific Heat, c_p	875	860	960	896
Failure Parameter 1, D_1	0.31	0.71	-0.068	-0.77
Failure Parameter 2, D_2	0.045	1.248	0.451	1.45
Failure Parameter 3, D_3	1.7	-1.42	-0.952	0.47
Failure Parameter 4, D_4	0.005	0.147	0.036	0
Failure Parameter 5, D_5	0	0	0.697	1.6

After these values are entered into the used analysis program, yield strength and plastic strain graphs are produced according to different strain rates. The graph formed for the Al2024-T3 alloy is given in Figure 7. As can be seen in the figure, the yield strength of the material increases as the strain rate increases. Therefore the behavior of our material changes in high-velocity impacts, and the behavior of the material must be modeled correctly in order to obtain accurate results.

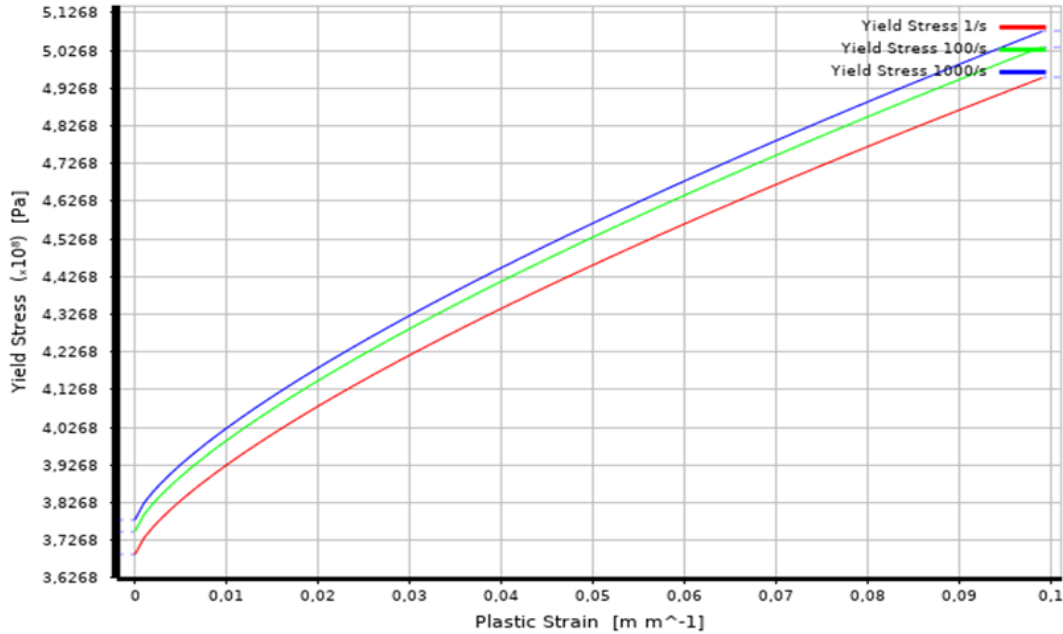


Figure 7: Yield strength-plastic strain graph for Al 2024-T3 alloy.







DESIGN OF EXPERIMENT

In a bird strike analysis, the system is affected by many factors. As the number of factors increases, the number of required experiments increases and the applications become more difficult. The Taguchi Method was used in the design phase of the bird strike experiment. Thus, a significant decrease in the number of experiments was observed as a result of the preliminary experiments.

Dr. Genichi Taguchi did a lot of important research with DOE techniques in the 1940s. Taguchi's experimental design approach was easier for users with limited statistical knowledge. As a result of these searches, he developed the Taguchi Method, which is easier to apply and used to make higher quality products. With the Taguchi Method, the integration of statistical methods into engineering studies can be done perfectly. For this reason, it has gained widespread popularity and has become more accepted in the engineering and scientific community. Another reason for adopting the Taguchi Method is its idea of creating superior manufacturing processes at much lower costs [Karna, 2012].

The factors and levels of this experimental design are given in Table 2. An experimental design was made according to these factors and levels and analyzes were carried out according to this experimental design.

Table 2: Factors and levels determined for design of experiment.

Factors	Levels					
	A1	A2	A3	A4	A5	A6
Leading Edge Designs						
Skin Material	Al2024-T3		Al7075-T6		Al7050-T7451	
Reinforcement Panel Material	Al2024-T3		Al7075-T6		Al7050-T7451	
Skin Thickness (mm)	1.2		1.4		1.6	
Reinforcement Panel Thickness (mm)	0.6		0.8		1.0	

RESULTS AND DISCUSSIONS

Validation of Bird Strike

Before performing bird strike analysis on complex structures used in aviation, it should be verified by comparing the results of previous experiments. For this comparison, bird strike experiments on simple flat plates and rigid plates were examined and compared with the analysis results. One of these experiments performed on a flat plate is Welsh's experiment [Welsh, 1986]. Welsh's experiment is schematically given in Figure 8. In the experiment, the experiment was performed with a dead chicken and gelatin bird model on the Al6061-T6 target plate. As a result of the experiment, the displacement in the flight direction at the midpoint of the aluminum plate was investigated. [Poola, 2011 and Mav, 2014] also used this experiment to validate their numerical analysis. In these studies, a fixed-support boundary condition is given on all four sides of the plate. To facilitate analysis, the plate is supported on all sides. In the experiment, the bird thrown at the 6.35 mm thick plate with a speed of 145.7 m/s caused a maximum displacement of 41.275 mm on the plate. Considering these conditions, a comparison study was made with the geometries given in Figure 5.

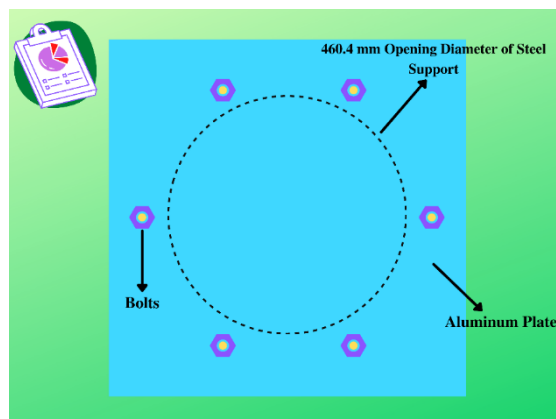


Figure 8: Schematic view of the experiment examined in the literature.

According to the results of the experiment, the geometry of the model bird to be used in the analysis was studied. Model bird geometries frequently used in previous studies are ellipsoid, hemispherical-ended cylinder, flat-ended cylinder, and spherical. In the experiment, the changes in the Al6061-T6 plate were compared with the high-impact velocities analyzes

consisting of different bird geometries in the analysis. All geometries except sphere had an aspect ratio of 2:1. Information about the geometry of the bird is given in Figure 9. In this comparison study, the bird was modeled by the SPH method and the element size was 5 mm. The plate mesh element size is 5 mm. The Johnson Cook material model was used to model the aluminum material and is taken from Table 1.

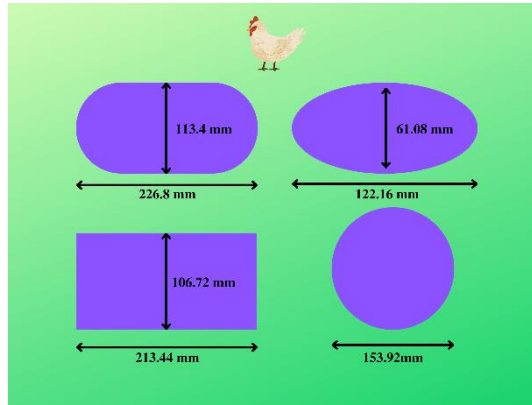
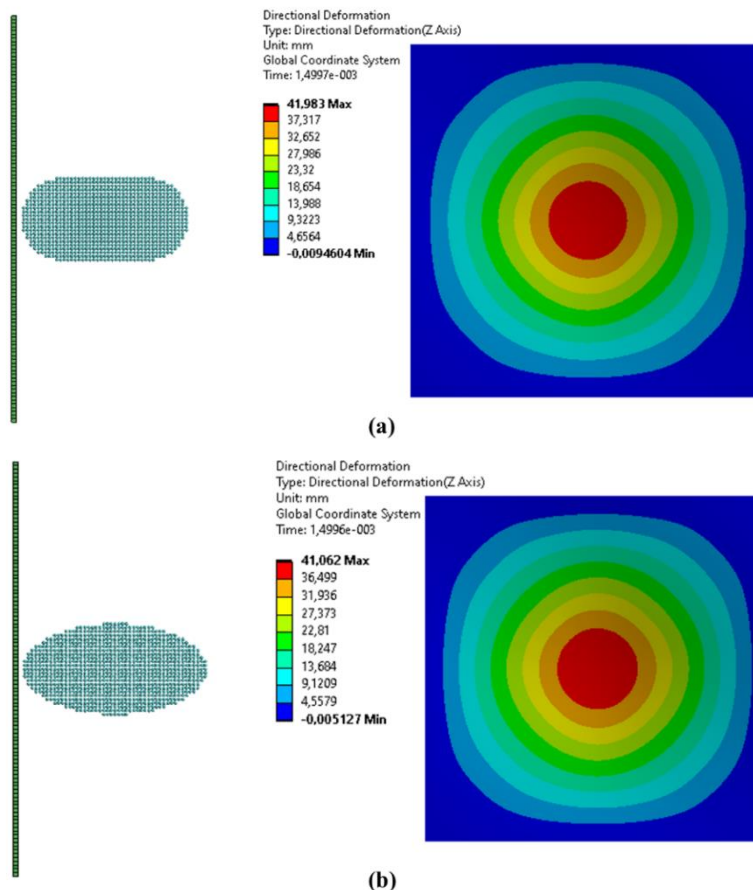


Figure 9: Dimension of bird impactor geometries in analysis.

Studies with different geometries in the analysis are given in Figure 10. When we look at the displacement change values at the midpoint of the plate, it is seen that the ellipsoid shape gives results closer to the value in the experiment. Bird models with ellipsoid shape and hemispherical-ended cylinder gave similar results. On the other hand, the spherical bird model caused the most damage and drifted away from the test result. The displacement-time graph of the plate obtained with different geometries is given in Figure 11. The displacement amount on the plate resulting from the spherical and flat-ended cylinder bird model showed a different movement compared to the other two geometries.



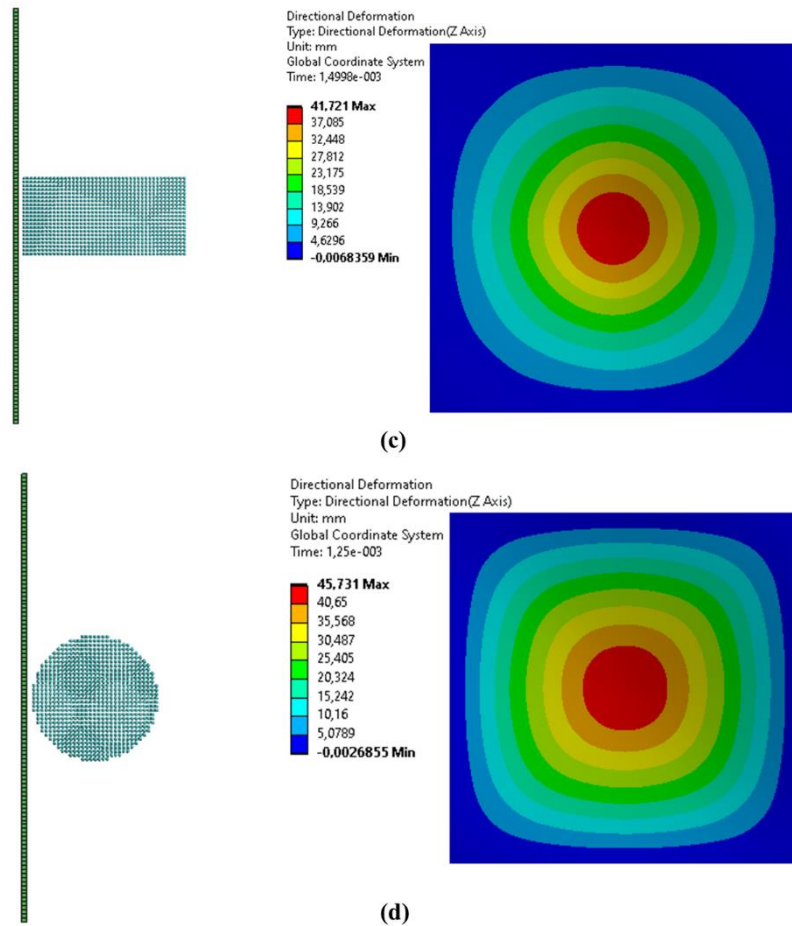


Figure 10: Displacement results according to different bird impactor shapes. (a) Hemispherical-ended cylinder bird model and results, (b) ellipsoid bird model and results, (c) flat-ended cylinder bird model and results, (d) spherical bird model and results.

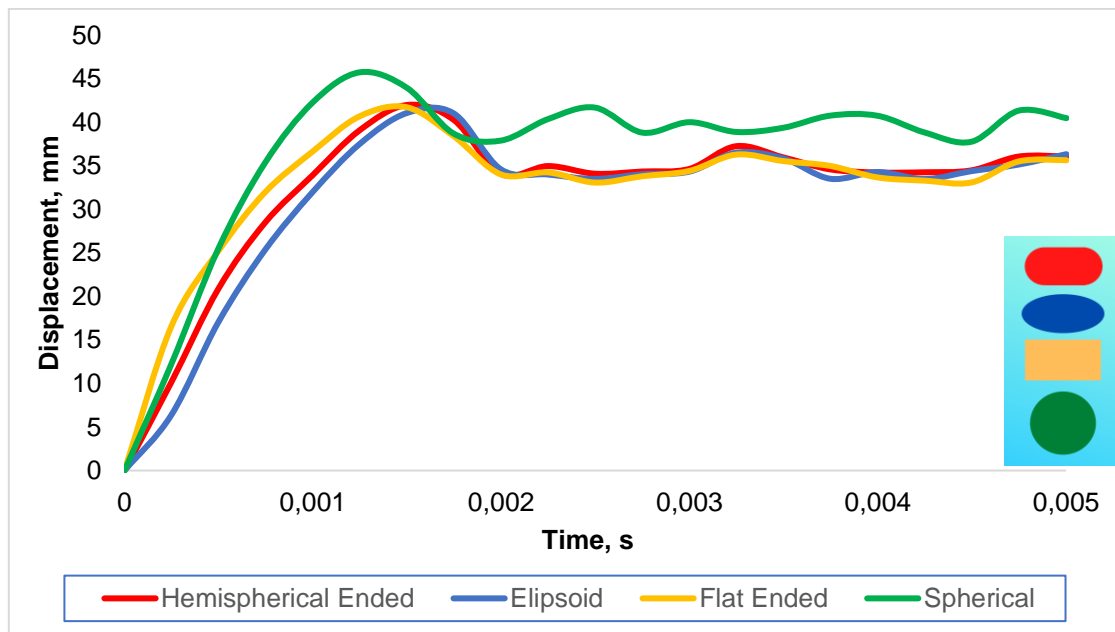


Figure 11: The amount of displacement on the plate with respect to time with different bird model geometries.

As seen in this analysis, the bird model with ellipsoid geometry gave a closer result. When we look at Figure 11, the behavior of the ellipsoid and hemispherical-ended cylinder bird model is very close to each other on the plate. However, since the most used and suggested geometry in previous studies was hemispherical-ended cylinder bird model, this geometry was used in later studies.

Determining the Optimum Wing Leading Edge Design

Different designs against bird strikes were examined in the literature and these designs were included in the experimental design. In addition, factors and levels were determined in the experimental design by considering the material and thickness of the leading edge skin and the support placed between the spar and the skin. In the Taguchi Method, the appropriate orthogonal array was chosen to design the experiment. This selected orthogonal array is in L18 ($6^1 3^4$) format. When all variables are taken into account, the Taguchi Method was used as there were too many situations to be analyzed and the situation that needed to be analyzed was kept to a minimum and eighteen different situations were examined. These different situations are given in Table 3. During the study, the velocity of the bird was taken as 77.2 m/s (150 knots).

Table 3: Design of experiment with L18($6^1 3^4$).

No. of Exp.	Design	Skin Material	Reinforcement Panel Material	Skin Thickness	Reinforcement Panel Thickness
1	A1	Al2024-T3	Al2024-T3	1.2 mm	0.6 mm
2	A1	Al7075-T6	Al7075-T6	1.4 mm	0.8 mm
3	A1	Al7050-T7451	Al7050-T7451	1.6 mm	1.0 mm
4	A2	Al2024-T3	Al2024-T3	1.4 mm	0.8 mm
5	A2	Al7075-T6	Al7075-T6	1.6 mm	1.0 mm
6	A2	Al7050-T7451	Al7050-T7451	1.2 mm	0.6 mm
7	A3	Al2024-T3	Al7075-T6	1.2 mm	1.0 mm
8	A3	Al7075-T6	Al7050-T7451	1.4 mm	0.6 mm
9	A3	Al7050-T7451	Al2024-T3	1.6 mm	0.8 mm
10	A4	Al2024-T3	Al7050-T7451	1.6 mm	0.8 mm
11	A4	Al7075-T6	Al2024-T3	1.2 mm	1.0 mm
12	A4	Al7050-T7451	Al7075-T6	1.4 mm	0.6 mm
13	A5	Al2024-T3	Al7075-T6	1.6 mm	0.6 mm
14	A5	Al7075-T6	Al7050-T7451	1.2 mm	0.8 mm
15	A5	Al7050-T7451	Al2024-T3	1.4 mm	1.0 mm
16	A6	Al2024-T3	Al7050-T7451	1.4 mm	1.0 mm
17	A6	Al7075-T6	Al2024-T3	1.6 mm	0.6 mm
18	A6	Al7050-T7451	Al7075-T6	1.2 mm	0.8 mm

The results of all experiments were examined according to the signal-to-noise ratio and the desired result was determined according to less mass and deformation. From the analysis study, the leading edge's condition before the impact is given in Figure 12 and the amount of displacement after the impact is given in Figure 13.

Analyzes were also made for other experiments, and the mass obtained and the maximum displacement at the leading edge are given in Table 4. These results were added to the outputs section of the Minitab program and signal-noise results were created. Signal-to-noise graphs were created with the "smaller-is-better" option, as the desired mass and displacement amounts for our leading edge design should be minimal.

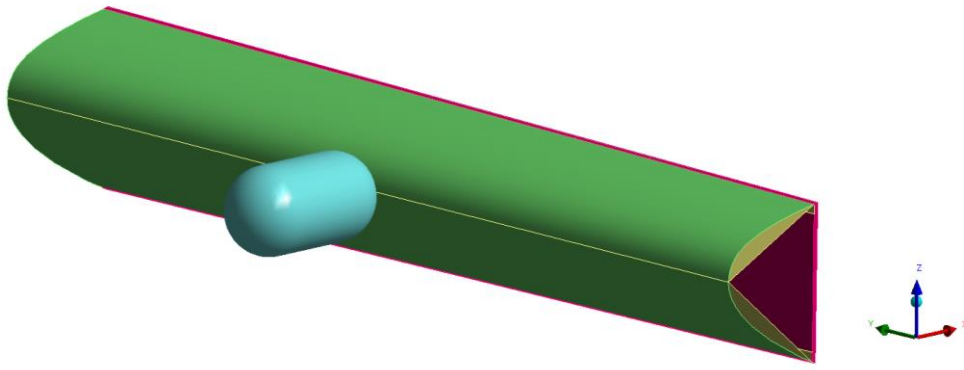


Figure 12: Leading edge before impact for Experiment #1.

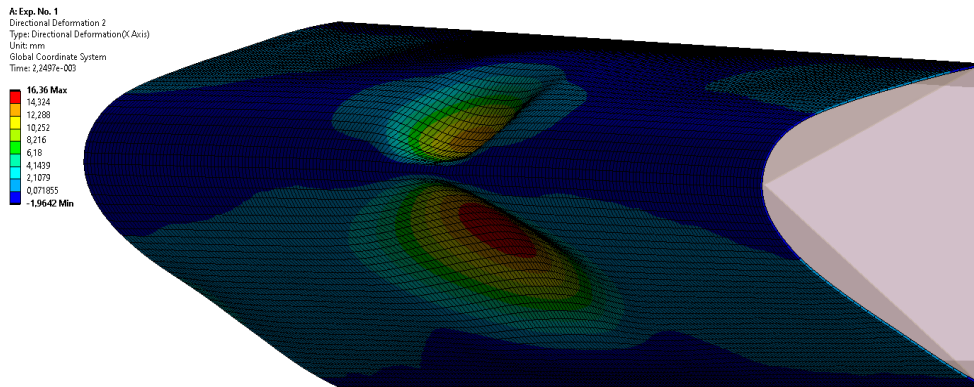


Figure 13: The amount of displacement and image of Experiment #1 after the impact.

Table 4: The results of the analysis studies carried out according to the experimental design.

Number of Experiment	Mass (kg)	Max. Displacement (mm)
1	4.01420	16.36000
2	4.41210	5.45150
3	4.80329	2.58180
4	3.99331	93.61100
5	4.29218	41.49100
6	3.75191	112.49000
7	3.96082	120.99000
8	3.97044	75.85400
9	4.26106	63.15800
10	4.36622	74.13000
11	4.12776	88.74300
12	4.07382	86.41600
13	4.27638	78.78400
14	4.26878	102.54000
15	4.39943	88.13000
16	4.25072	101.94000
17	4.27372	54.62800
18	3.99679	117.09000

The signal-to-noise ratio graphs obtained according to the results of the analyzes are given in Figure 14 and 15. Figure 14 is the graph obtained for mass. According to this chart, the minimum mass level for the leading edge can be reached by choosing the combination of A2 for the appropriate design geometry, Al2024-T3 for the skin material, 7075-T6 for the panel material, 1.2 mm for the surface thickness, and 0.6 mm for the panel thickness. Looking at the intervals in the graph, it is seen that the factors affecting the mass the most are design, skin, and support thickness.

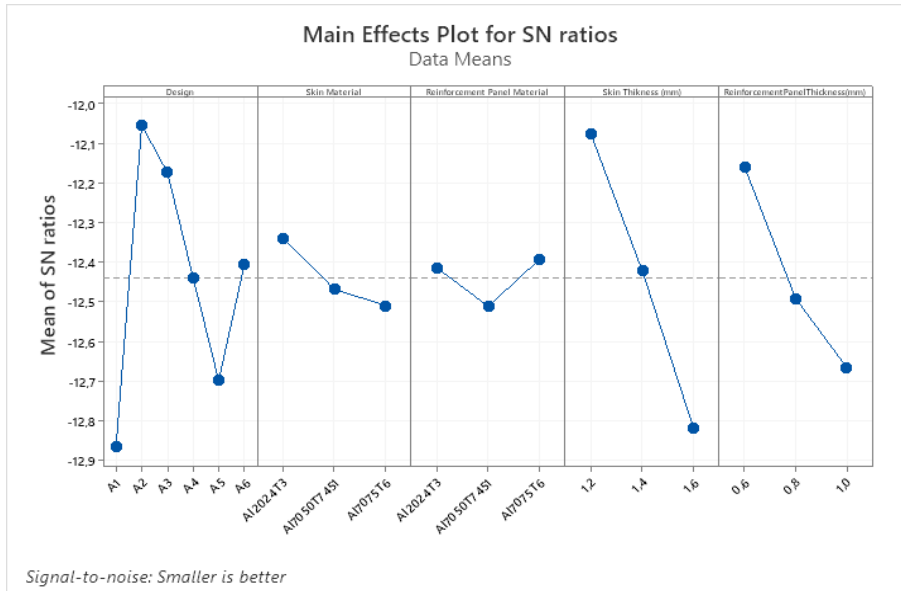


Figure 14: Signal-to-noise ratio for mass versus design, skin material, panel material, skin thickness, and panel thickness.

The signal-to-noise ratio graph obtained for the deformation of the skin is given in Figure 15. According to this graph, the deformation that may occur in the leading edge skin can be minimized by taking the combination of A1 for the appropriate design geometry, Al7075-T6 for the skin material, Al7050-T7451 for the panel material, 1.6 mm thick of the skin material and 1 mm for the panel thickness. Looking at this graph, it is seen that the most influential factor on deformation is design and skin thickness.

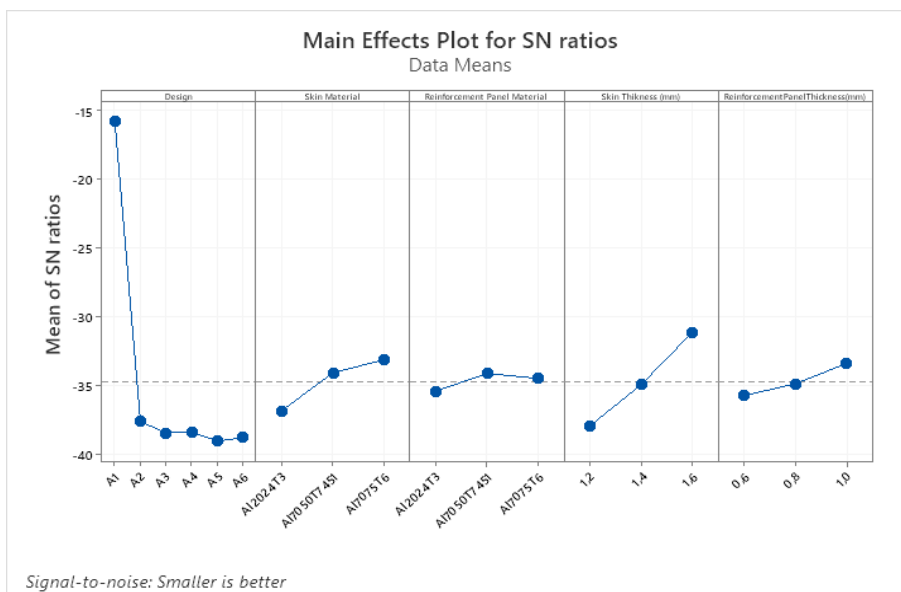


Figure 15: Signal-to-noise ratio for displacement of leading edge skin versus design, skin material, panel material, skin thickness, and panel thickness.

Figure 16 is the graph obtained for mass and displacement. According to this graph, the best performance can be achieved by choosing the combination of A1 for the appropriate design geometry, Al7075-T6 for skin and panel material, 1.6 mm for skin thickness and 1.0 mm for panel thickness.

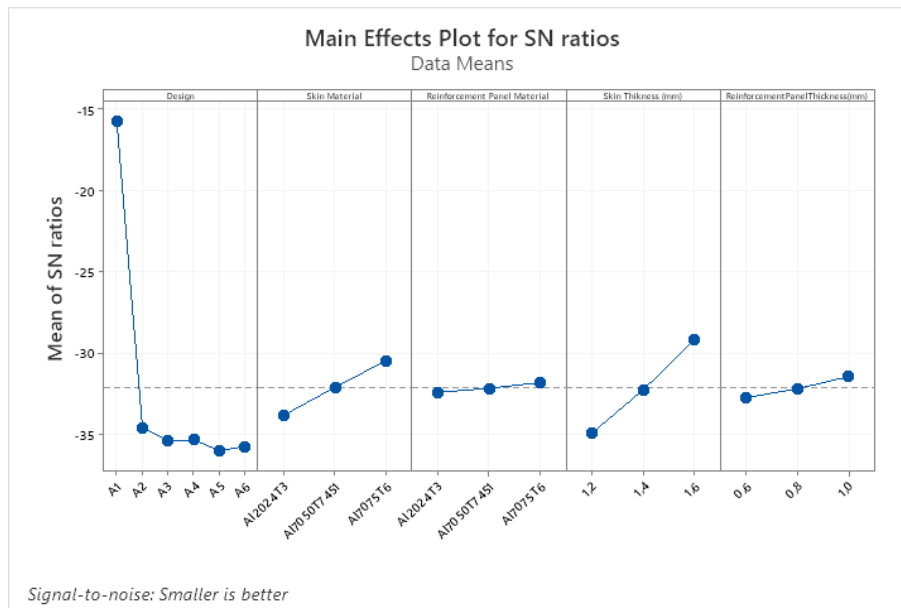


Figure 16: Signal-to-noise ratio for mass and displacement of leading edge skin versus design, skin material, panel material, skin thickness, and panel thickness.

CONCLUSION

In this project, bird strikes at the leading edge of the aircraft wing were investigated. Bird strike is a serious problem in aviation, it causes loss of life and property. Within the scope of the project, the experiments carried out in the field of bird strike from past to present have been examined and the methods used have been investigated. Firstly, the experiment made on a flat aluminum plate was examined by simulation method and when compared with the results in the experiment, close values were obtained. During this review, the bird geometries proposed in the past were studied and it was observed that the ellipsoid model gave closer results. However, since the hemispherical-ended cylinder model is the most used and recommended geometry in the past studies, the hemispherical-ended cylinder model was used in the study process. Different designs have been made in the past to provide the wing leading edges with minimal damage from bird strikes. Considering these designs, skin and panel thickness, skin and panel materials, an experimental design was made with the Taguchi Method. As a result of this experimental design, the combination giving the least mass and deformation was chosen and these results were decided by looking at the signal-to-noise ratio. Considering the graphics obtained, it was seen that the most important parameters for the mass and deformation, which are the performance requirements, are the design geometry and the skin thickness.

ACKNOWLEDGEMENT

This work is supported both by The Scientific and Technological Research Council of Turkey (TÜBİTAK) under 2209-B program and Turkish Aerospace Industries, Inc., under Lift-Up program. Both institutions are profoundly acknowledged.

References

- Allan, John R., "The Costs of Bird Strikes and Bird Strike Prevention" (2000). Human Conflicts with Wildlife: Economic Considerations. 18.
- Aluminum 7050-T7451 Retrieved March 20, 2021
<http://www.matweb.com/search/DataSheet.aspx?MatGUID=142262cf7fbc4c83917ca5c3d17df1ed>.
- Aurrekoetxea, M., López de Lacalle, L. N., & Llanos, I. (2020). *Machining Stresses and Initial Geometry on Bulk Residual Stresses Characterization by On-Machine Layer Removal*. Materials, 13(6), 1445.
- Brar, N. & Joshi, V. & Harris, B. (2009). *Constitutive Model Constants for Al7075-T651 and Al7075-T6*. AIP Conference Proceedings. 1195. 10.1063/1.3295300.
- Budgey, Richard. (2000). *The Development of a Substitute Artificial Bird by The International Bird Strike Research Group for Use in Aircraft Component Testing*. International Bird Strike Committee ISBC25/WP-IE3, Amsterdam.
- Buyuk, M. (2013). *Development of a Tabulated Thermo-Viscoplastic Material Model with Regularized Failure For Dynamic Ductile Failure Prediction of Structures Under Impact Loading* (Doctoral dissertation, The George Washington University).
- Dolbeer, R. A., Begier, M. J., Miller, P. R., Weller, J. R., & Anderson, A. L. (2019). *Wildlife Strikes to Civil Aircraft in the United States, 1990–2019* (Rep.). Federal Aviation Administration.
- Frequently asked questions and answers. (2020, August 28). Retrieved February 24, 2021, from https://www.faa.gov/airports/airport_safety/wildlife/faq/
- Hedayati, R., & Sadighi, M. (2016). *Bird strike: An Experimental, Theoretical and Numerical Investigation*. Amsterdam: Elsevier, WP Woodhead Publishing.
- Hedayati, R., & Ziaei-Rad, S. (2013). *A New Bird Model and The Effect of Bird Geometry in Impacts from Various Orientations*. Aerospace Science and Technology, 28(1), 9–20.
- Heimbs, S. (2011). *Computational Methods for Bird Strike Simulations: A Review*. Computers & Structures, 89(23-24), 2093–2112.
- Huang, X., Xu, J., Chen, M., & Ren, F. (2020). *Finite Element Modeling of High-Speed Milling 7050-T7451 Alloys*. Procedia Manufacturing, 43, 471–478.
- Karna, S. K. (2012). *An Overview on Taguchi Method*. International Journal of Engineering and Mathematical Sciences, 11–18.
- Mav, R.K. (2014). *Numerical Analysis of Bird Strike Damage on Composite Sandwich Structure Using Abaqus / Explicit*.
- Milani, A. S., Dabboussi, W., Nemes, J. A., & Abeyaratne, R. C. (2009). *An Improved Multi-Objective Identification of Johnson-Cook Material Parameters*. International Journal of Impact Engineering, 36(2), 294–302. <https://doi.org/10.1016/j.ijimpeng.2008.02.003>
- Nicholson, R., & Reed, W. S. (2011). *Strategies for Prevention of Bird Strike Events*. AERO, (Issue 43 _Quarter 03)
- Poola, R. (2011). *Bird Strike Impact Analysis of Vertical Stabilizer Structure Using Abaqus/Explicit*.
- Sumesh, C. S., & Ramesh, A. (2018). *Numerical Modelling and Optimization of Dry Orthogonal Turning of Al6061 T6 Alloy*. Periodica Polytechnica Mechanical Engineering, 62(3), 196–202.

Velamakuri, N. S. C., Myers, O. J., & Wyatt, J. E. (2018). *Numerical Analysis Conducted During the Study on the Impact of Tool-Chip Contact Time on the Shear Angle in Orthogonal Machining*. *International Journal of Metallurgy and Metal Physics*, 3(1), 1–16.

Welsh, C., & Centonze, V. (1986). *Aircraft Transparency Testing - Artificial Birds*.